Molecular Biology of the Cell
Vol. 9, 1037–1051, May 1998

# Nuclear Ferritin Protects DNA From UV Damage in Corneal Epithelial Cells

**Cindy X. Cai, David E. Birk, and Thomas F. Linsenmayer***

Department of Anatomy and Cellular Biology, Tufts University Medical School, Boston, Massachusetts 02111

Submitted August 4, 1997; Accepted February 24, 1998
Monitoring Editor: Keith Yamamoto

Previously, we identified the heavy chain of ferritin as a developmentally regulated nuclear protein of embryonic chicken corneal epithelial cells. The nuclear ferritin is assembled into a supramolecular form indistinguishable from the cytoplasmic form of ferritin found in other cell types and thus most likely has iron-sequestering capabilities. Free iron, via the Fenton reaction, is known to exacerbate UV-induced and other oxidative damage to cellular components, including DNA. Since corneal epithelial cells are constantly exposed to UV light, we hypothesized that the nuclear ferritin might protect the DNA of these cells from free radical damage. To test this possibility, primary cultures of cells from corneal epithelium and stroma, and from skin epithelium and stroma, were UV irradiated, and DNA strand breaks were detected by an in situ 3′-end labeling method. Corneal epithelial cells without nuclear ferritin were also examined. We observed that the corneal epithelial cells with nuclear ferritin had significantly less DNA breakage than other cell types examined. Furthermore, increasing the iron concentration of the culture medium exacerbated the generation of UV-induced DNA strand breaks in corneal and skin fibroblasts, but not in the corneal epithelial cells. Most convincingly, corneal epithelial cells in which the expression of nuclear ferritin was inhibited became much more susceptible to UV-induced DNA damage. Therefore, it seems that corneal epithelial cells have evolved a novel, nuclear ferritin-based mechanism for protecting their DNA against UV damage.

## INTRODUCTION

DNA is a major target of UV-induced cellular damage. All three wavelengths of naturally occurring UV light, UV-A, B, and C (200–400 nm), may directly induce pyrimidine and thymine dimer formation, DNA strand breaks, and DNA–protein cross-linking. UV-induced DNA damage then stimulates signal transduction pathways, resulting in either repair and cell survival or cell death (Liu *et al.*, 1996). It is thought that UV-induced skin cancer may largely result from such DNA damage (Hart *et al.*, 1977). In this respect, cornea is very different from skin. Primary cancers of corneal epithelial cells are extraordinally rare even though this tissue is transparent and constantly exposed to UV light (Smolinand and Thoft, 1987). This raises the possibility that corneal epithelial cells may have evolved one or more defense mechanisms to prevent damage to their DNA.

UV irradiation can also indirectly damage cells through the formation of active oxygen species (AOS) (Yamanashi *et al.*, 1979; Black, 1987; Shimmura *et al.*, 1996). The resulting oxidative damage (Halliwell and Aruoma, 1991) can be mutagenic and may also be involved in carcinogenesis (Cerutti, 1985). Free iron has been shown to catalyze the formation of UV-induced AOS via the Fenton reaction (Stohs and Bagchi, 1995). Thus, the concentration of intracellular free iron is tightly regulated and kept at a low level, chiefly by the iron-sequestering action of the ferritin that is found in the cytoplasm of most cells.

We have recently observed that ferritin is a developmentally regulated nuclear protein in avian corneal epithelial cells (Cai *et al.*, 1997). Results from both immunohistochemical analyses and subcellular frac-

* Corresponding author.

tionation are consistent with this conclusion. Of the tissues examined in vivo, the nuclear localization of ferritin is highly selective for corneal epithelium. In vitro, however, nuclear localization can be induced in certain other cell types by manipulating the iron concentration of the culture medium.

Immunoblotting of corneal epithelial extracts showed that the nuclear ferritin has a supramolecular structure indistinguishable from that of the cytoplasmic ferritin found in other cell types (Cai *et al.*, 1997). This suggests that nuclear ferritin can bind iron. Cytoplasmic ferritin, by sequestering free iron, has been shown to function as an antioxidant (Balla *et al.*, 1992). Since corneal epithelial cells are constantly exposed to environmental AOS-generating $O_2$ and UV light, we asked whether in this cell type, the nuclear ferritin might serve a protective function in preventing damage to DNA, and possibly other nuclear components. To test this hypothesis, in the present studies, we examined, by an in situ 3′-end labeling method, the effect of nuclear ferritin in decreasing the UV-induced DNA strand breaks. Of the cell types examined, corneal epithelial cells, with nuclear ferritin, were the least sensitive to UV-induced DNA damage. Moreover, elevated iron exacerbated the generation of UV-induced DNA strand breaks in fibroblasts from cornea and skin, but not in corneal epithelial cells. Most importantly, corneal epithelial cells in which the appearance of nuclear ferritin had been blocked showed more DNA damage than did those with nuclear ferritin. These results are all consistent with the proposition that in this cell type, nuclear ferritin protects DNA against UV damage.

## MATERIALS AND METHODS

### *Cell Cultures*

UV irradiation was performed on primary cell cultures grown in two-chamber glass slides (Falcon, Lincoln Park, NJ). Corneas, or pieces of skin, were separated into epithelial and stromal components by treatment in 0.5% Dispase for 1 h at 4°C (Spurr and Gipson, 1985). The epithelial cell sheets were rinsed in PBS and then further digested in 0.25% trypsin at 37°C for 5 min. The stromal fibroblasts were separated by further digestion in a 1:1 mixture of trypsin (0.25%) and collagenase (200 U/ml) for 2 h at 37°C. All cells were cultured in a complete medium (normal medium) consisting of a 1:1 mixture of DMEM [Fe $(NO_3)_3$ level ~ 0.1 $\mu$g/ml or 0.25 $\mu$M] and F-12 nutrient medium ($FeSO_4$ level ~ 0.83 $\mu$g/ml or 3 $\mu$M) (Life Technologies/BRL, Gaithersburg, MD), 20% FCS (heat-inactivated, total iron ~ 1 $\mu$g/ml, 50% saturation of total iron binding capacity of serum transferrin) (Hyclone, Logan, UT), 1% chicken serum (Life Technologies/BRL), 5 $\mu$g/ml insulin (Sigma Chemical, St. Louis, MO), 10 ng/ml human recombinant EGF and penicillin and streptomycin (Life Technologies/BRL). The total iron concentration in this medium is ~ 0.6 $\mu$g/ml. Cultures were maintained for 38–42 h before UV irradiation.

For some studies, the iron concentration in the culture medium was increased by the addition of ferrous sulfate (100–200 $\mu$M, Sigma). Primary cells were incubated for 48 h in normal medium before being changed to this high-iron medium for another 16 h before UV irradiation. In some studies, ferritin expression was inhibited by adding the iron chelator deferoxamine (100 $\mu$M, Sigma) to the culture medium. After 24–48 h, the deferoxamine-containing medium was replaced with either normal medium or high-iron medium, and the cells were cultured for an additional 14–16 h before UV irradiation. As a control for possible toxicity of the chelator, other cultures were treated with equimolar concentrations of deferoxamine and ferrous sulfate.

### *UV Irradiation*

The cells were exposed to 254 nm UV light generated by a Stratalinker UV Crosslinker (model 1800: power level ~3000 $\mu$W/cm$^2$) (Stratagene, La Jolla, CA) using the "time mode" of operation. The complete medium on each slide chamber was replaced with 1 ml of DMEM, and the slides were then placed on ice and UV irradiated. Control cells were treated identically except that they were exposed to ambient fluorescent light rather than UV light. After the treatments, fresh culture medium containing 15 $\mu$M aphidicolin, an inhibitor of DNA replication, was added, and the cells were returned to the incubator for an additional 1, 2, 4, or 8 h before fixation.

### *Detection of UV-induced DNA Strand Breaks*

UV-induced strand breaks were detected by an in situ 3′-end labeling method (ISEL) (Bromidge *et al.*, 1995; Coates *et al.*, 1995). The cells in two-chamber slides were fixed in fresh 4% paraformaldehyde (30 min) and permeabilized in 0.4% Triton X-100, 0.1% sodium citrate (20 min). Then they were incubated at 37°C for 1 h in 50 $\mu$l of 1× terminal deoxynucleotide transferase reaction buffer containing 0.2 M potassium cacodylate, 25 mM Tris-HCl, 0.25 mg/ml of BSA (Boehringer Mannheim, Indianapolis, IN), 2.5 mM cobalt chloride (Boehringer Mannheim), 10 $\mu$M biotin-14-deoxycytidine triphosphate (Life Technologies/BRL) and 12.5 U of terminal transferase (Boehringer Mannheim). The cultures were washed in 1× PBS and then were incubated in tetramethylrhodamine-conjugated streptavidin (Molecular Probes, Sunnyvale, CA) (50 $\mu$l of a 10 $\mu$g/ml solution diluted in PBS) at 37°C for 30 min. They were then washed and mounted in glycerol/PBS (95:5) containing 1 $\mu$g/ml Hoechst dye No. 33258 (Sigma). They were viewed with a Nikon fluorescence photomicroscope, and photographs were taken with Kodak TMAX 400 film at a 1-min exposure time. For quantitation, the photographs were scanned and the digitized images were analyzed using UTHSCSA Image Tool Software Package, Version 1.27.

### *Immunofluorescence Cytochemistry*

Cells were fixed in cold 4% paraformaldehyde (10 min), further fixed in cold 2% methanol (5 min), and permeabilized with cold 100% methanol (10 min). They were incubated for 30 min at 37°C in 50 $\mu$l of antiferritin monoclonal antibody 6D11 (5 $\mu$g/ml) (Zak and Linsenmayer, 1983; Cai *et al.*, 1997), or, as a control, monoclonal antibody X-AC9, against type X collagen (Schmid and Linsenmayer, 1985).The samples were then washed in PBS and incubated with a rhodamine-conjugated goat anti-mouse secondary antibody. After washing in PBS, the samples were mounted and viewed as described above.

## RESULTS

To examine whether the nuclear ferritin within the corneal epithelial cells confers protection against UV damage, we irradiated primary cell cultures with UV light, and then evaluated DNA strand breaks by ISEL. The cell types tested were epithelial cells and fibroblasts from embryonic day 12–14 corneas and from day 7–8 skin. Day 12–14 corneal tissues were chosen

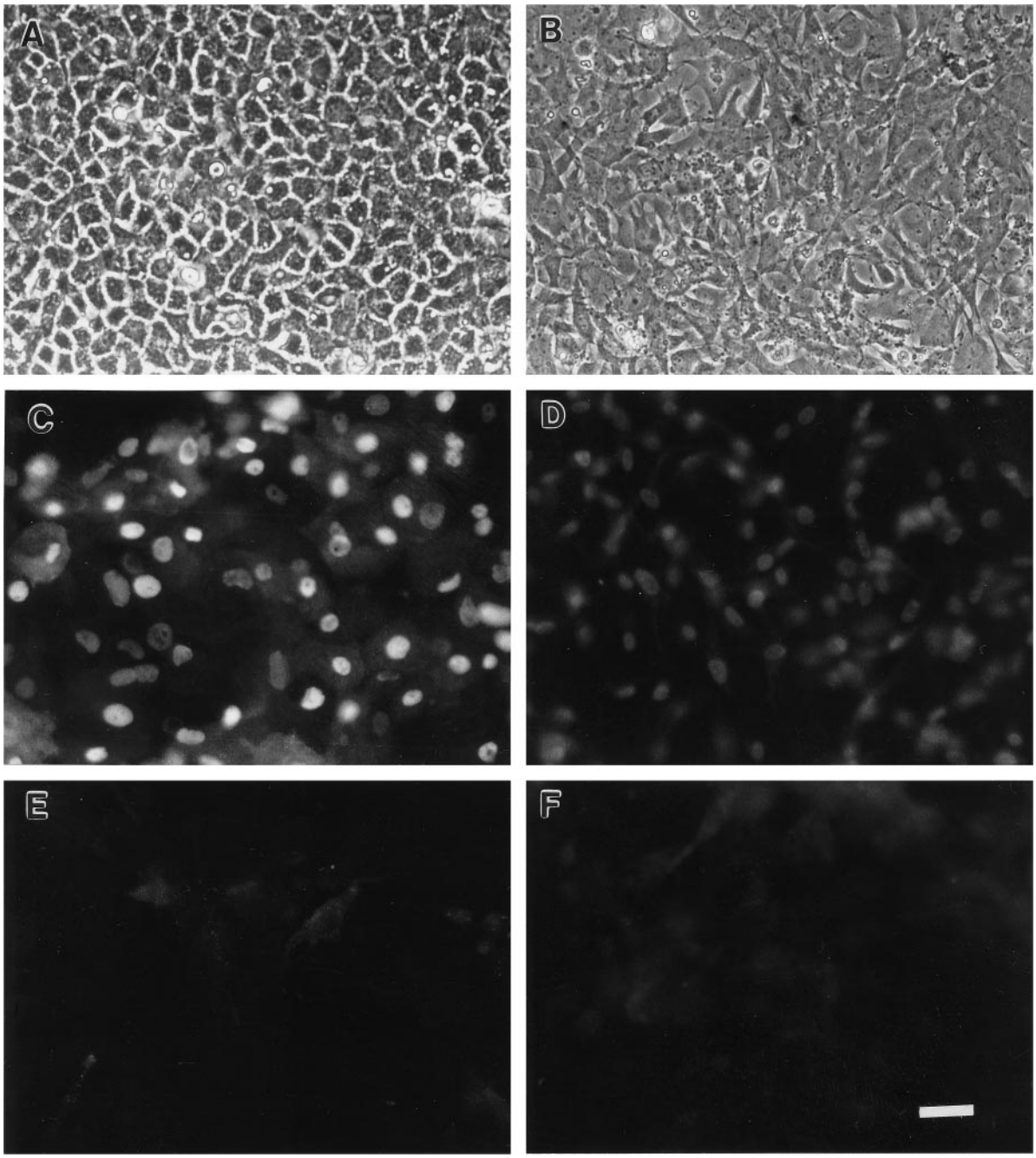


**Figure 1.** Micrographs of primary cultures of 14-d corneal epithelial cells (A and C) and corneal fibroblasts (B and D), and 8-d skin epithelial cells (E) and skin fibroblasts (F). Panels A and B are phase contrast. Panels C–F are immunofluorescence micrographs of cells reacted with the anti-chick ferritin monoclonal antibody 6D11. Bar, 25 $\mu$m.

since nuclear ferritin had already appeared in the epithelium by that stage (Cai *et al.*, 1997); 7- to 8-d skin was used since appreciable feather development had not yet occurred (7- to 8-d corneal epithelial cells will be discussed later).

The epithelial cells from cornea and skin had a similar polygonal morphology and growth in a sheet (Figure 1A). They showed limited proliferation, could not be passed, and began to deteriorate after 7 d in culture. Thus, they were cultured for only 38–42 h before being used for experimentation. Fibroblasts, on the other hand, had an elongated shape (Figure 1B) and could undergo several passages without noticeable phenotypic changes. Consistent with our previous

studies (Cai *et al.*, 1997), the corneal epithelial cells were the only ones with a high level of nuclear ferritin (Figure 1C). Some corneal fibroblasts showed a low level of nuclear ferritin (Figure 1D) (although they had none in vivo [Cai *et al.*, 1997]), and skin epithelial cells (Figure 1E) and fibroblasts (Figure 1F) showed little, if any, in the nucleus and low levels in the cytoplasm.

### *Dose-dependent UV-induced DNA Damage*

In all experiments, positive and negative controls were included to monitor the efficiency of ISEL detection, both among the different cell types within each experiment, and between experiments. As a positive control, a sample of each cell type was treated with DNase I (9 $\mu$g/ml, 37°C for 15 min) to induce DNA strand breaks. All cell types thus treated produced a strong nuclear signal by ISEL. As a negative control, cells were treated identically as the experimental samples, except that they were exposed to ambient fluorescent light.

All cell types showed the generation of UV-induced DNA strand breaks in a dose-dependent manner. This can be seen for the corneal epithelial cells and corneal fibroblasts in Figure 2, and has also been reported for other cell types in other species (Pitts *et al.*, 1987; Bromidge *et al.*, 1995).

The corneal epithelial cells, however, were by far the most resistant. In this cell type only 17% of the cells showed a detectible ISEL signal when exposed to UV irradiation for 5 min (total energy = 970 mJ/cm$^2$) and examined 2 h later (Figure 2, CE 5′ and quantitation panel solid bar). Even within this small population, the signal in most of these cells (69%) was only marginally detectable (solid line in quantitation panel). The remaining 31% of this population showed a strong signal (arrows in CE 5′ and solid line in 5′ quantitation). However, their characteristically small nuclei suggest that they mainly represent a background level of cell death in the cultures, since small, strongly positive nuclei were also observed in the UV-negative controls (CE, UV-; solid line and bar in UV- quantitation).

With the same 5-min treatment, 97% of the corneal fibroblasts were ISEL positive (CF 5′ and hatched bar in quantitation), and the average signal intensity was much stronger (dashed line in 5′ quantitation).

As can be seen in the 8- and 11-min panels in Figure 2, with progressive increases in exposure time, more corneal epithelial cells showed positive signals (91.5% with 8 min [1.44 J/cm$^2$] and 98.5% with 11 min [1.98 J/cm$^2$]), and the relative intensities of the signals increased (see quantitation panels). In comparison, with 8 min exposure, all of the corneal fibroblasts were positive and remained so with 11 min exposure. More importantly, their signal intensities were much greater—frequently reaching the maximum level that could be measured (dashed lines in quantitation panels). The majority of the non–UV-irradiated cells (UV−) showed little labeling, except for the occasional small nuclei mentioned above.

The skin epithelial cells were noticeably more sensitive than corneal epithelial cells to UV irradiation, showing obvious nuclear labeling with 5 min of irradiation (our unpublished results, but see below). The sensitivity of skin fibroblasts was indistinguishable from that of the corneal fibroblasts (our unpublished results).

When the UV exposure was increased to 20 min (our unpublished observations), all of the cells in all cell types were strongly labeled. With even longer exposures, the nuclear signal showed no increase, suggesting that the 20-min exposure had produced the maximum amount of UV-induced breakage that could be detected by this method.

### *Temporal Appearance of UV-Induced DNA Damage*

We next examined whether temporal differences exist in the appearance of UV-induced DNA damage. For this, cells were exposed to 5 min of irradiation (total energy = 970 mJ/cm$^2$) and then were examined by ISEL at 1 and 4 h later. To minimize the potential influence of DNA repair, the DNA polymerase inhibitor aphidicolin (Gedik *et al.*, 1992) was included in the culture medium added after the UV irradiation.

In corneal epithelial cells, the appearance of UV-induced DNA breaks was clearly retarded when compared with the cell types that had little or no nuclear ferritin. In the corneal and skin fibroblasts, DNA breaks could be detected throughout the population as early as 30 min after irradiation (our unpublished results), and after 1 h ~95% of the cells of both types were positive, as shown in Figure 3 (1 h CF and SF) and Figure 4 (striped and hatched bars). At the same 1-h time point, fewer skin epithelial cells showed damage (Figure 3, SE), but the number was still an appreciable 35% (Figure 4, open bar), while only 12% of the corneal epithelial cells showed damage (Figure 4, solid bar), and at least some of these were the previously mentioned cells with the small nuclei (Figure 3, 1 h CE). At 2 h after exposure (our unpublished observations), the corneal epithelial cells were indistinguishable in the number of positive cells and the signal intensity from those at 1 h, whereas all the other cell types showed stronger labeling than at 1 h.

In the corneal epithelial population, it was not until 4 h after UV exposure that the number of positive cells began to rise, to 44% (Figure 4, solid bar), and among these the intensities of the signal varied (Figure 3, CE, 4 h). This suggested heterogeneity within the population, possibly reflecting variations in the level of nuclear ferritin, as shown in later experiments. At this time point, double the number of skin epithelial cells

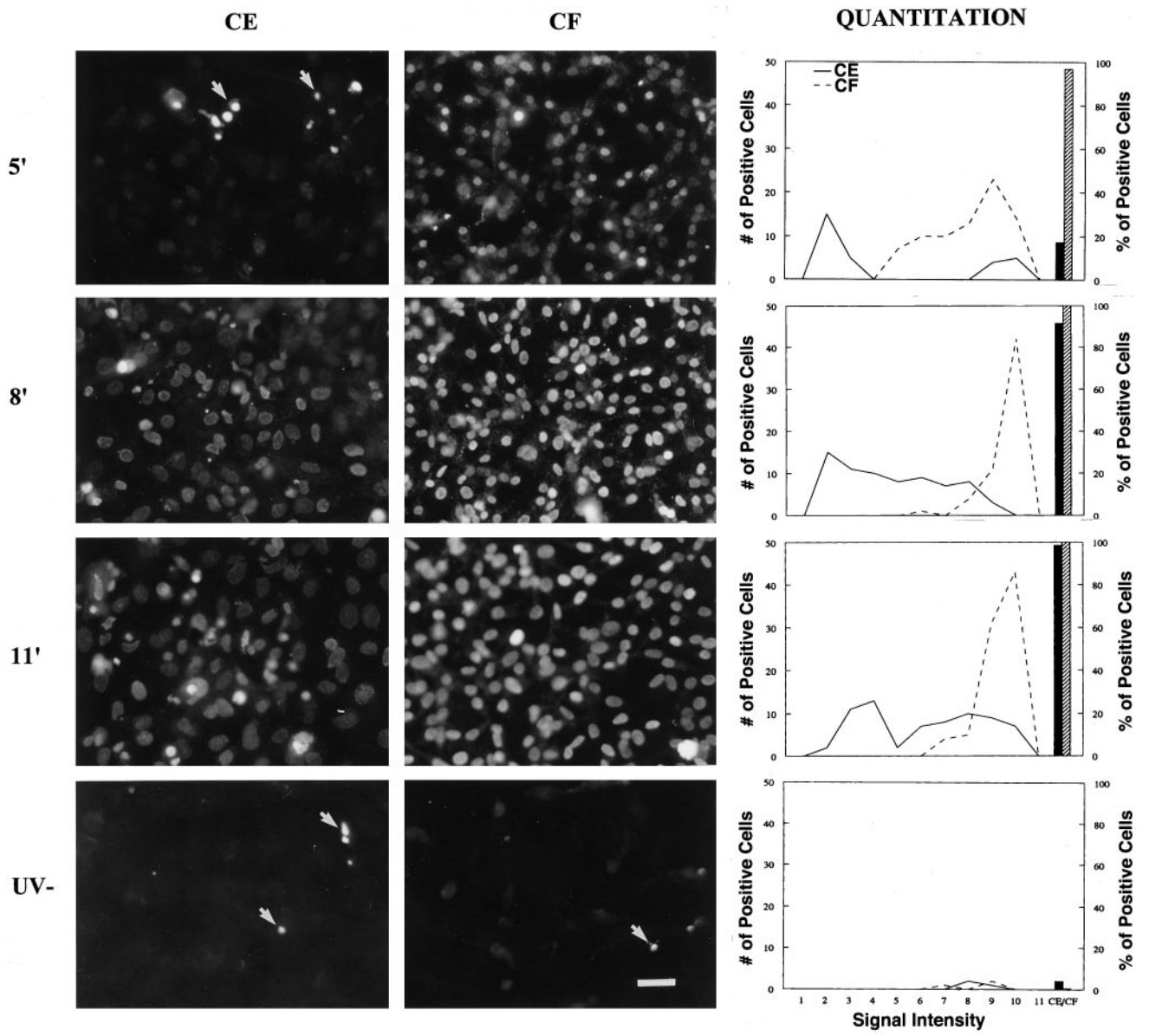


**Figure 2.** Fluorescence micrographs of 14-d corneal epithelial cells (CE) and corneal fibroblasts (CF) exposed to UV light for 5 min, 8 min, and 11 min and processed 2 h later for ISEL visualization of DNA breakage. Negative controls (UV−) were exposed to ambient light for 5 min. The arrows show the small strongly labeled nuclei found both in the experimental and control samples. Also presented in the panels labeled "Quantitation" are the percentages of ISEL-positive cells (bar graphs: CE, solid bars; CF, hatched bars) and the distributions of the relative signal intensities of these cell (line graphs: solid lines, CE; dashed lines, CF). The signal intensities were determined from digitized images (using the UTHSCSA Image Tool 1.27 software program), and then data were plotted as mean gray scale values from 20–260 U, in increments of 20 U. Bar, 25 $\mu$m.

(83%) were positive (Figure 4, empty bar), and the signal in these was uniformly intense (Figure 3, SE, 4 h). Some skin epithelial cells also showed nuclear condensation and fragmentation (arrows), which could be seen in Hoechst dye-stained preparation (our unpublished observations). In the corneal and skin fibroblasts at 4 h, 100% of the cells were positive cells (Figure 4, striped and hatch bars). The signal was similarly intense at 1 h, suggesting that at 1 h the maximum level of detection by this method had already been reached. There were, however, other differences in the nuclei at 4 h, including an overall decrease in their number, and an increase in those with a shrunken and/or condensed morphology. These are characteristics of UV-induced cell death, as also reported by others (Lu and Lane, 1993).

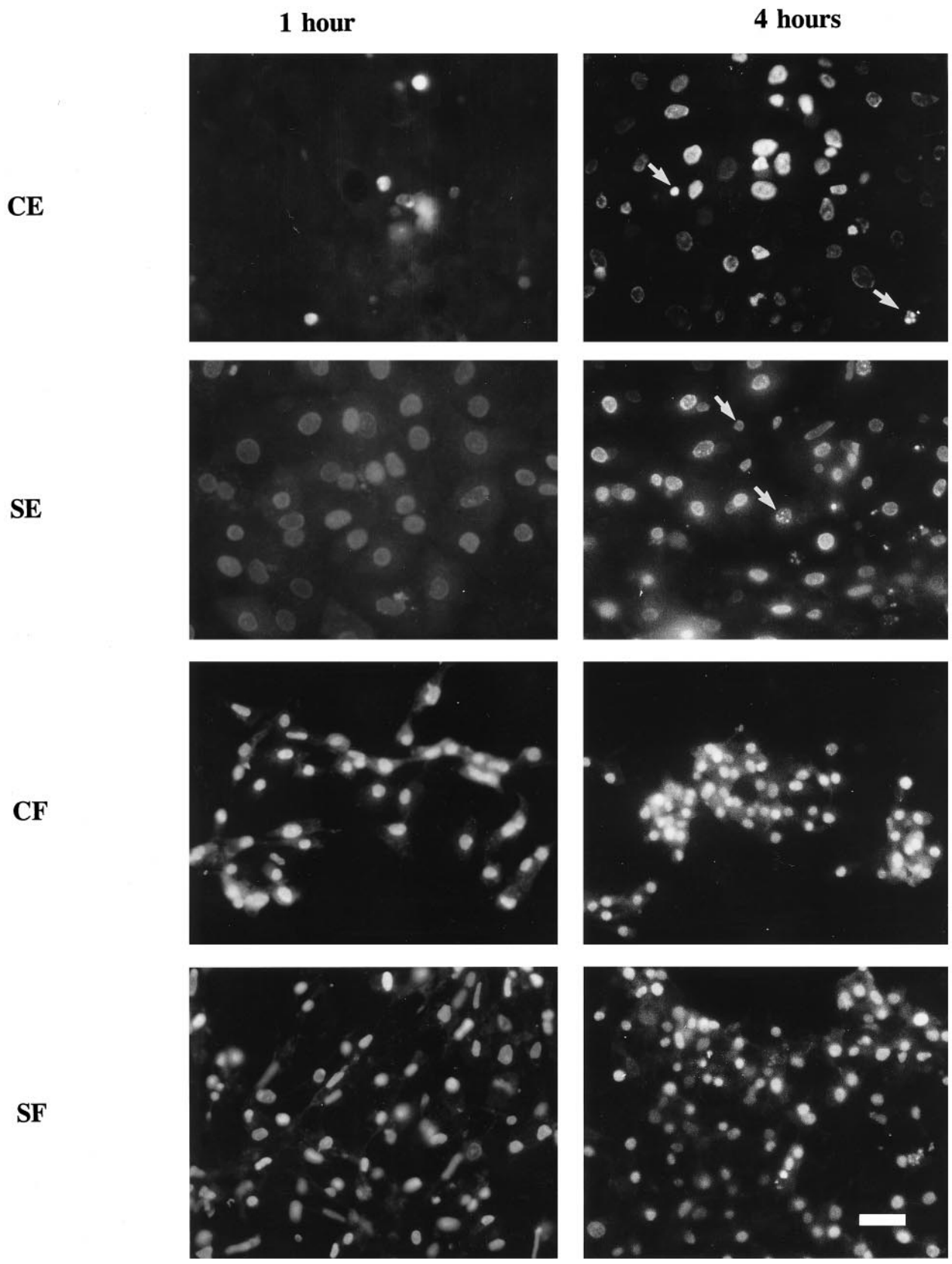


**Figure 3.**

By 8 h (our unpublished observations), except for the corneal epithelial cells, all cell types showed major cell loss. The overall appearance of the corneal epithelial population was similar to that at 4 h, except that some cells showed a slight increase in the ISEL signal and a few showed nuclear fragmentation.

### *Effects of Lower Dosage Irradiation on Different Cell Types*

We also examined the effect of lower doses of UV radiation on these cell types. Since the experiments just described showed that the maximum detectable ISEL signal was reached by 4 h postirradiation, we used this time point to examine the effects of lower doses of radiation (Figure 5).

Corneal epithelial cells with either a 2-min exposure (total energy = 360 mJ/cm$^2$) or a 3-min exposure (total energy = 540 mJ/cm$^2$) showed little if any nuclear labeling (CE, 2 min and 3 min) when compared with the nonirradiated cells (our unpublished observations). Even when these cells were exposed for 4 min (total energy = 720 mJ/cm$^2$), the majority of the cells still had no labeling (CE, 4 min). However, the 4-min exposure did reveal a subpopulation of cells that seemed hypersensitive, some even showing nuclear fragmentation (arrows).

The skin epithelial cells were much more sensitive, showing a strong ISEL signal and some nuclear fragmentation after only 2 min of exposure (SE, 2 min). With 3- and 4-min exposures (SE, 3 min and 4 min), stronger signals and more nuclear fragmentation were observed. Corneal fibroblasts showed only weak ISEL signals with 2 and 3 min of exposure (CF, 2 min and 3 min), but with a 4- min exposure almost all cells showed strong labeling (CF, 4 min). The responses of skin fibroblasts with either a 2-min or a 4-min exposure (SF, 2 min & 4 min) were indistinguishable from the corneal fibroblasts with those treatments. The intermediate, 3-min exposure (SF, 3 min), however, revealed a subpopulation of cells that were more sensitive, again possibly reflecting a heterogeneity in nuclear ferritin.

### *Effects of Elevated Iron on UV-induced DNA Damage*

All of these experiments suggested that corneal epithelial cells have a cell-type-specific defensive mechanism(s) preventing UV-induced DNA damage. This, coupled with studies by others suggesting that increased iron exacerbates UV-induced DNA damage (Audic and Giacomoni, 1993; Stohs and Bagchi, 1995), raised the possibility that the nuclear ferritin might be involved in this protection.

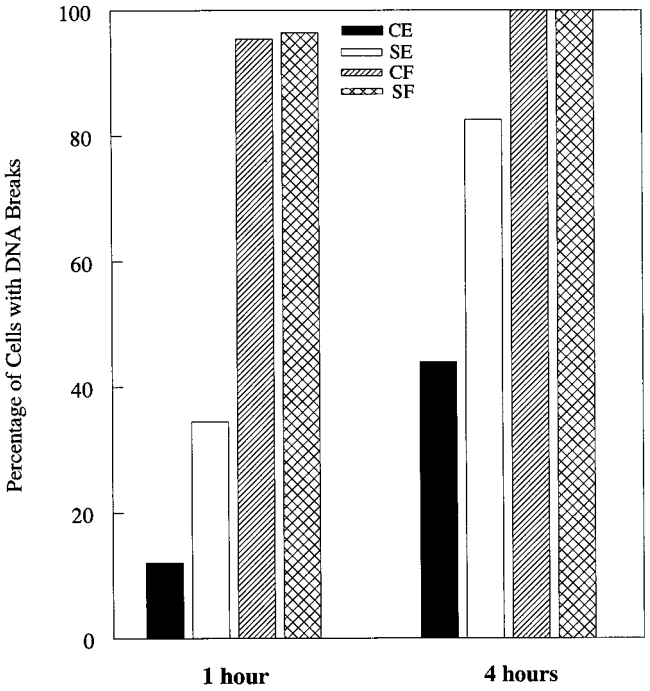


**Figure 4.** Quantitation of the percentages of cells showing UV-induced DNA breaks at 1 and 4 h after 5 min of UV irradiation (see micrographs in Figure 3) in populations of corneal epithelial cells (solid bars), skin epithelial cells (empty bars), corneal fibroblasts (striped bars), and skin fibroblasts (hatched bars).

First, we examined the effect of increased iron. For this, corneal epithelial cells and fibroblasts from 12- to 14-d corneas, and epithelial cells and fibroblasts from 7- to 8-d skin, were cultured for 48 h in normal medium (iron level ~ 0.6 $\mu$g/ml). Then they were transferred into high-iron medium, which consisted of normal medium supplemented with either 100 $\mu$M (27.8 $\mu$g/ml) or 200 $\mu$M (55.6 $\mu$g/ml) ferrous sulfate. After 16 h of incubation in high-iron media, the cells were UV irradiated for 5 min and examined 4 h later by ISEL.

The nuclear ferritin content of the corneal epithelial cells, as estimated by immunofluorescence, was similar in both high-iron medium (Figure 6A) and normal medium (compare with Figure 1C). Consistent with our previous studies (Cai *et al.*, 1997), however, in high-iron medium, corneal fibroblasts (Figure 6B) and skin fibroblasts (our unpublished observations) showed increased cytoplasmic ferritin when compared with cells in normal medium (Figure 1D). In some fibroblasts from both tissues, ferritin was also now found in the nucleus (arrows), but in general, this

**Figure 3 (facing page).** Fluorescence micrographs of 12-d corneal epithelial cells (CE), 8-d skin epithelial cells (SE), 12-d corneal fibroblasts (CF), and 8-d skin fibroblasts (SF) reacted for DNA breaks by ISEL. The cells were exposed to UV light for 5 min and then were fixed at 1 h and 4 h after treatment. Arrows indicate the labeling of small nuclei or nuclear fragmentation. Bar, 25 $\mu$m.

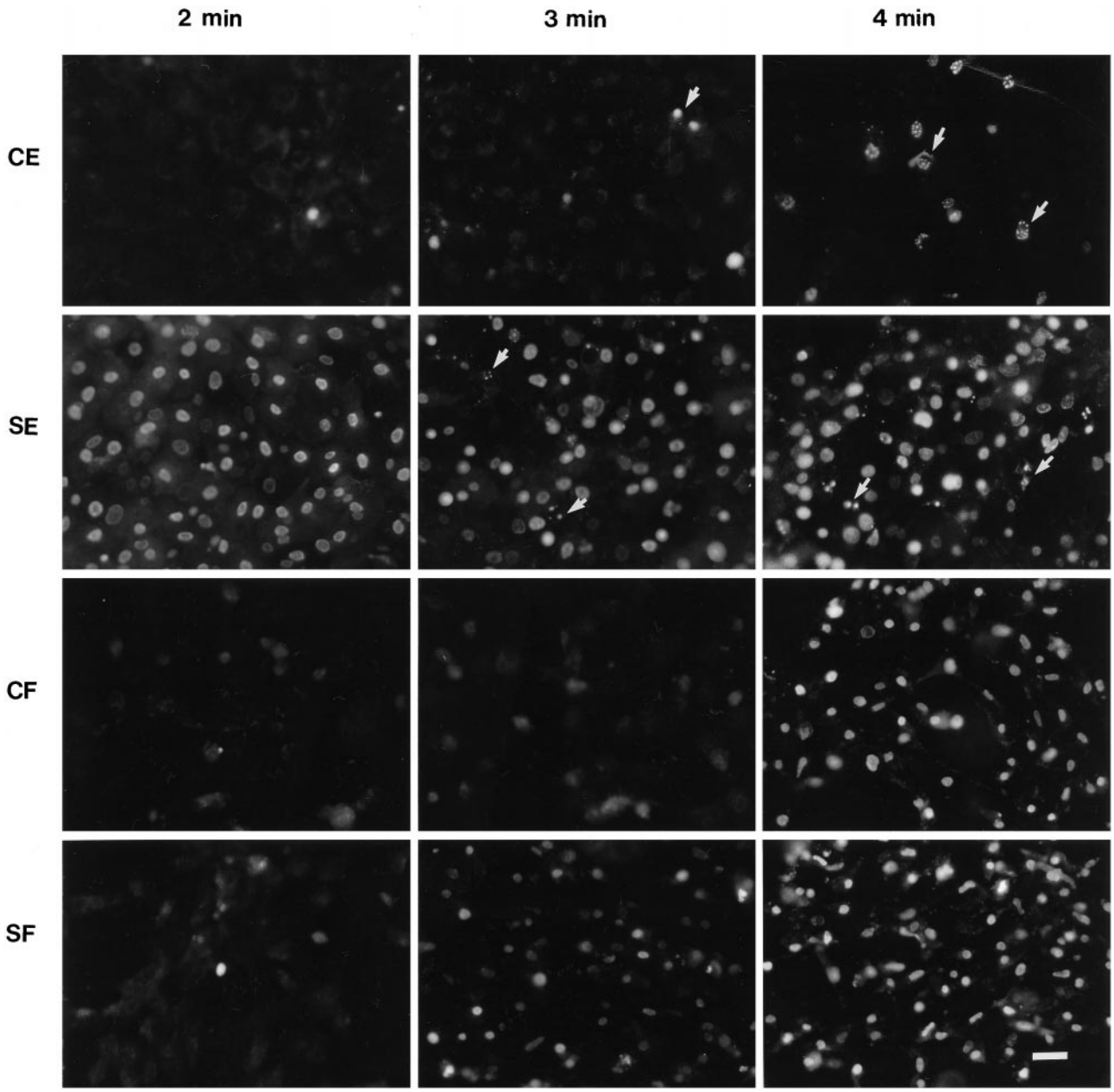


**Figure 5.** Fluorescence micrographs of 12-d corneal epithelial cells (CE), 8-d skin epithelial cells (SE), 12-d corneal fibroblasts (CF), and 8-d skin fibroblasts (SF) exposed to UV irradiation for 2, 3, and 4 min and examined for DNA breaks by ISEL 4 h later. The 4-min exposure induced strong nuclear labeling for DNA breaks in all the cell types tested, except for corneal epithelial cells, in which only occasional fragmented nuclei showed strong labeling (arrows). Bar, 25 $\mu$m.

was at a lower level than in the nuclei of the corneal epithelial cells.

In normal medium, 3 min of irradiation produced little detectable damage to the DNA of either the corneal epithelial cells (Figure 6C) or the corneal fibroblasts (Figure 6D). This was also true for the corneal epithelial cells in high-iron medium (Figure 6E). The corneal fibroblasts in high-iron medium, however, showed a large increase in the ISEL signal (Figure 6F), as was also true for skin fibroblasts (our unpublished observations).

Skin epithelial cells (our unpublished observations), when placed in high-iron medium, also showed elevated ferritin. However, this was mostly in the cytoplasm. Exposure of these cells to UV irradiation resulted in their subsequent detachment from the

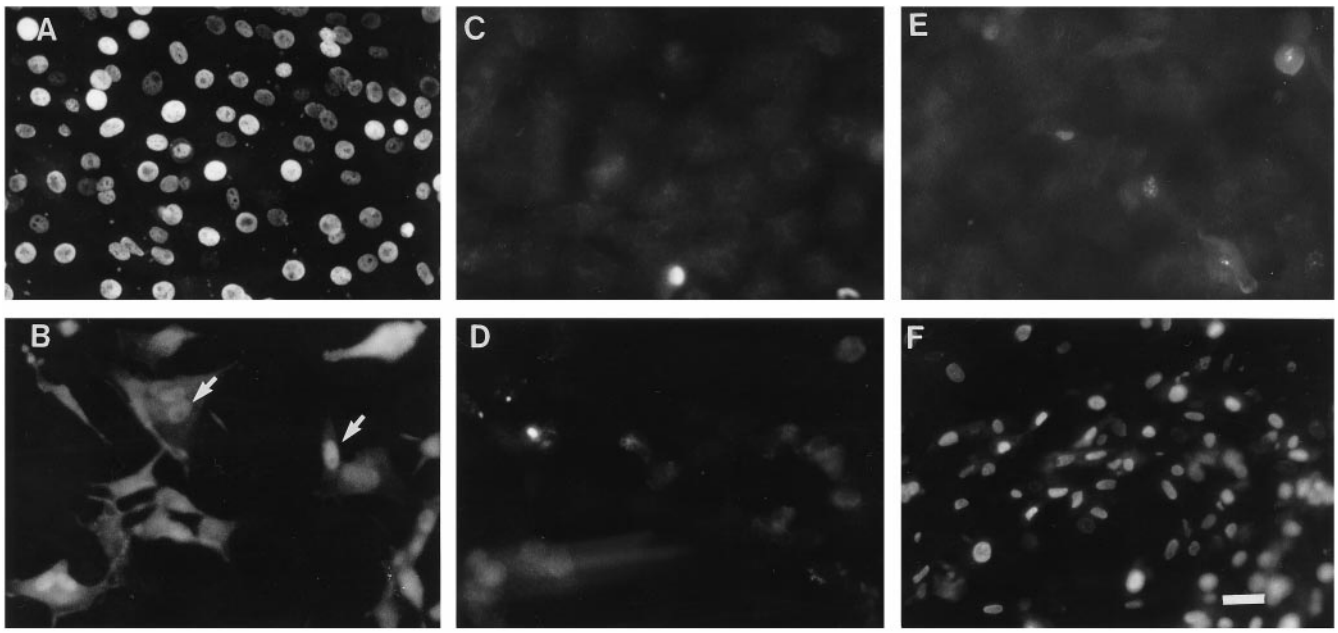


**Figure 6.** Fluorescence micrographs of 12-d corneal epithelial cells (A, C, and E) and corneal fibroblasts (B, D, and F) cultured in normal (C and D) or high-iron medium (100 $\mu$M ferrous sulfate) (A, B, E, and F) for 16 h before a 3-min UV exposure. The cells were processed 4 h later for either ferritin localization or DNA breaks by ISEL. Panels A and B are the immunofluorescence micrographs of cells reacted for ferritin with monoclonal antibody 6D11. In the fibroblasts, both nuclear (arrows in panel B) and cytoplasmic immunoreactivity was observed. Panels C, D, E, and F are the micrographs of cells examined for DNA breakage by ISEL. Bar, 25 $\mu$m.

surface of the culture chamber slide. While this behavior precluded analysis by ISEL, it also suggested that the cells had suffered severe damage. This is consistent with the high UV sensitivity of this cell type, observed in the experiments described earlier.

These results suggest that in the corneal epithelial cells the nuclear ferritin can block or prevent UV-induced DNA damage. However, in the corneal and skin fibroblasts, the cytoplasmic ferritin and the low level of nuclear ferritin are inadequate to confer protection, as is also true for the cytoplasmic ferritin in the skin epithelial cells.

### *Increased UV-induced DNA Damage in Corneal Epithelial Cells without Nuclear Ferritin*

Our previous studies (Cai *et al.*, 1997) showed that during embryonic development, nuclear ferritin appeared in corneal epithelial cells in vivo at 11–12 d. However, when corneal epithelial cells from embryos as young as 7 d were put into culture, by 16 h they had expressed nuclear ferritin. This precocious expression of nuclear ferritin could be blocked by the iron chelator deferoxamine, suggesting that free iron in the medium was responsible —most likely by translational regulation (Cai *et al.*, 1997). We have now observed that this inhibition of ferritin expression by deferoxamine can be reversed by transferring the cells to a normal medium or high-iron medium. These manipulations have allowed us to test directly whether it is the nuclear ferritin that is responsible for preventing UV damage.

First, we examined more carefully the parameters of the in vitro repression and induction of the nuclear ferritin. Consistent with our previous results, when 7- to 8-d corneal epithelial cells were cultured in the presence of 100 $\mu$M deferoxamine for 24–48 h, the precocious expression of nuclear ferritin was inhibited (our unpublished observations, but see Pendrys [1983]). When cells were plated in the control medium (normal medium supplemented with equimolar concentrations of deferoxamine and ferrous sulfate), nuclear ferritin was expressed, demonstrating both the specificity of the iron chelator and its lack of toxicity.

In the deferoxamine-treated cultures, the expression of nuclear ferritin could be initiated by replacing the chelator-containing medium with either normal medium or high-iron medium. The kinetics of expression of the nuclear ferritin, however, were different in the two media. In the normal medium, the appearance was slow. At 15–18 h in this medium, $<$5% of the cells showed detectable ferritin, and at 26 h 13% showed expression. In the high-iron medium, recovery was faster. At 15 h, 20% of the cells had nuclear ferritin, although the amount per cell was variable; and at 18 h 50% of the cells were positive. In addition, the intensity of the ferritin signal in high-iron cultures was

much stronger than that in the normal cultures. In control cells treated with equimolar concentrations of deferoxamine and ferrous sulfate, 85% of the cells were positive. Using these manipulations, we were able to compare UV-induced DNA damage in corneal epithelial cells with no detectable nuclear ferritin, to cells that had partially recovered nuclear ferritin and to cells with a high level of nuclear ferritin.

To ensure that the deferoxamine treatment itself would not produce a difference in UV susceptibility, corneal epithelial cells were cultured for 48 h in either deferoxamine, or equimolar deferoxamine plus ferrous sulfate, UV-irradiated, and 4 h later examined by ISEL. In neither type of culture should appreciable free iron exist within the cells. In the deferoxamine-containing cultures, the iron would be chelated by the deferoxamine itself, and in the deferoxamine plus ferrous sulfate it would be chelated by the nuclear ferritin. After UV irradiation, no differences in DNA damage could be detected between the two types of cultures (our unpublished results).

When the cells in the two groups were transferred to normal medium for 16 h, dramatic differences in the extent of UV-induced damage between the groups were now observed. As can be seen in Figure 7A (solid bars), in the groups treated with deferoxamine (<5% ferritin positive cells), 67% of the cells showed signals for DNA breaks. In contrast, in the control groups treated with deferoxamine plus ferrous sulfate (>85% ferritin positive cells), only 13% of the cells showed DNA breaks. Furthermore, the ISEL signal produced by the cells without nuclear ferritin was visibly much stronger (Figure 7B, panel A) than that in the cells with the molecule (Figure 7B, panel C). There was also more nuclear fragmentation in the cells without ferritin (Figure 7B, arrows in panels A and B), as was also seen with Hoechst staining (compare Figure 7B, panels B and D).

We also tested for protection from UV-induced DNA breaks by ferritin under high-iron conditions. For this, corneal epithelial cells (treated with either deferoxamine or deferoxamine plus ferrous sulfate) were transferred to high-iron medium (as described above) for 16 h before UV-irradiation. Again, the cells that had been cultured in deferoxamine showed more damage than those that had been cultured in deferoxamine plus ferrous sulfate (77% for deferoxamine-treated cells and 31% for the controls) (Figure 7A, hatched bars). As compared with the results just described for the normal medium, both groups cultured in the high-iron medium showed a somewhat increased percentage of cells positive for DNA damage. This confirmed the involvement of iron in the damage process.

In addition, after 16 h in the high-iron medium, 20% of the cells in the deferoxamine group had initiated the expression of nuclear ferritin. This afforded the opportunity to examine whether this newly synthesized nuclear ferritin could protect cells from nuclear damage, even under the high-iron conditions.

To test this, individual corneal epithelial cultures were examined by triple labeling for ferritin (by immunofluorescence with a fluorescein-labeled secondary antibody), DNA breakage (by ISEL with a rhodamine-labeled reporter), and total cells (by DNA staining with Hoechst dye). The results were examined either as individual color channels (Figure 8A, panels a–c; and Figure 8B, panels a, b, d, and e), or, to facilitate comparison of the reactions, representative photographs were digitized and the colors superimposed (Figure 8B, panels c and f).

Consistent with the predictions, in many areas examined, there was essentially a complete separation between the cells with nuclear ferritin (Figure 8A, panel a) and those showing DNA damage (Figure 8A, panel b).Thus, most of the cells with nuclear ferritin showed little or no nuclear signals for DNA breaks.

In occasional areas, some overlap in the signals was observed. Two of these are shown in Figure 8B (panels a–c and d–f). Even in these selected areas, however, most of the cells with appreciable nuclear ferritin showed little, if any, nuclear signal for DNA damage (and thus appear green in the composite panels c and f). The cells with little or no ferritin, however, showed some DNA damage (and thus appear red or orange in these composite panels). Cells with weaker signals for nuclear ferritin have stronger signals for DNA breaks (for example, the cell demarcated by the thin arrows in panels a–c) and vice versa (in these panels, the cell demarcated by the thick arrows). Only occasionally did a cell show appreciable signals for both nuclear ferritin and for DNA breaks (for example, the cell demarcated by the arrows in panels d–f).

## DISCUSSION

The results reported here are all consistent with nuclear ferritin functioning as an agent responsible for protecting avian corneal epithelial cells from UV-induced DNA damage. Of the four cell types tested, the corneal epithelial cells, with nuclear ferritin, were the least susceptible to UV-induced DNA damage, as determined by ISEL and nuclear fragmentation. Iron stimulation exacerbated UV-induced DNA damage in all cell types tested, except for the ferritin-containing corneal epithelial cells. Most convincingly, cells in which the expression of nuclear ferritin was inhibited showed a large increase in DNA damage. Thus, avian corneal epithelial cells seem to have evolved a specific, nuclear ferritin-based mechanism of protecting their DNA against UV damage.

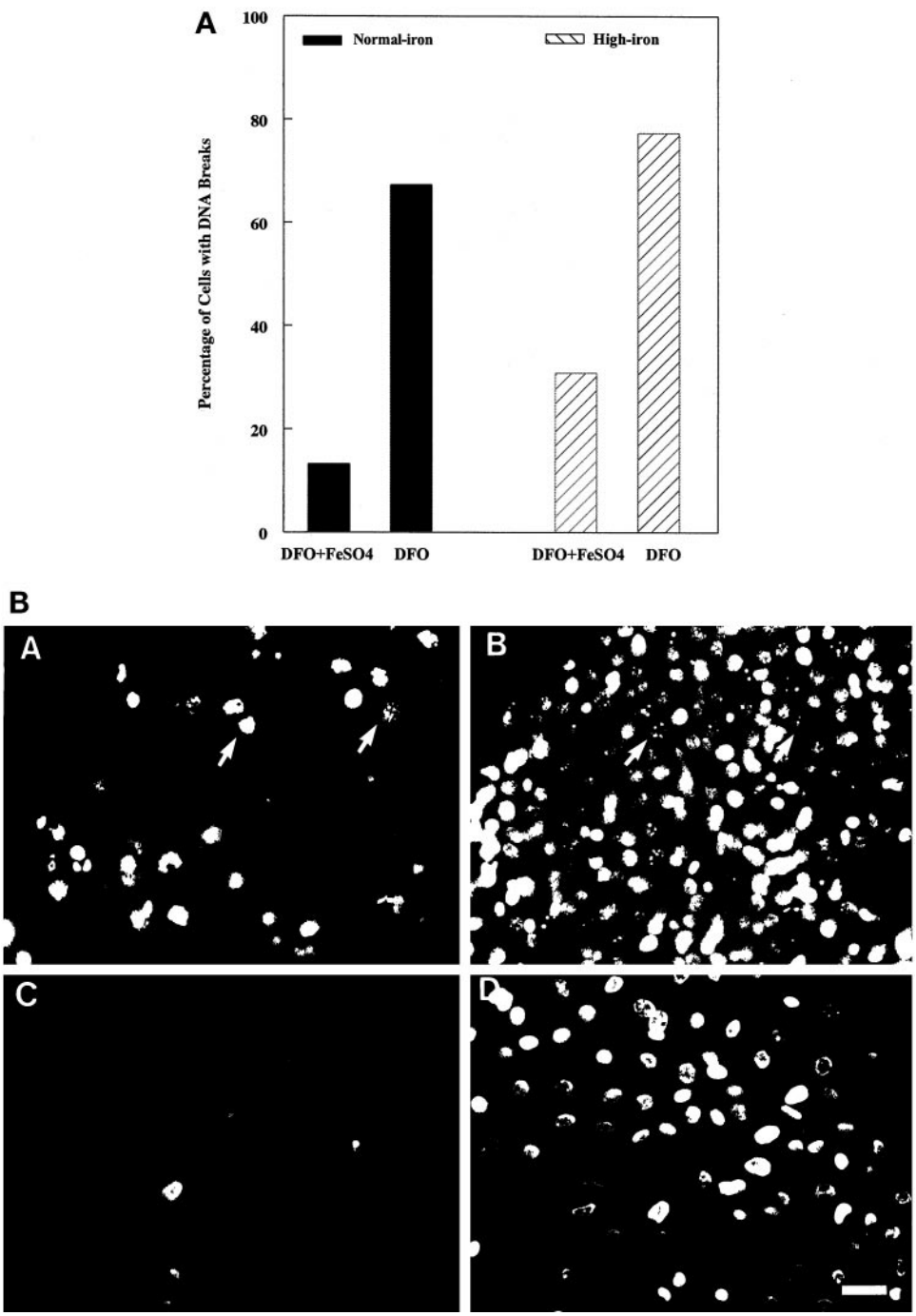


**Figure 7.** (A) (top panel), Quantitation of UV-induced DNA breaks in day 7–8 corneal epithelial cells treated with 100 $\mu$M deferoxamine (DFO) or equimolar concentrations of deferoxamine and ferrous sulfate (DFO+$FeSO_4$). Both groups of cells were cultured for an additional 16 h in normal-iron medium (solid bars) or high-iron medium (hatched bars). They were then exposed to UV light for 5 min and fixed 4 h later. The quantitative data were derived by averaging the percentage of positive cells for DNA breaks from two separate experiments. (B) (bottom panel), Fluorescence micrographs of 8-d corneal epithelial cells examined for DNA breakage by ISEL (A and C), and by Hoechst staining (B and D). The cells were treated either with deferoxamine (100 $\mu$M) (A and B) or equimolar concentrations of deferoxamine and ferrous sulfate (C and D) for 48 h. They were then incubated in normal-iron medium for an additional 16 h before exposure to 5 min of UV irradiation and fixation 4 h later. In the deferoxamine-treated cells, stronger ISEL signals and more nuclear fragmentation were observed (A, arrows), as also seen in Hoechst staining (B, arrows). Bar, 25 $\mu$m.

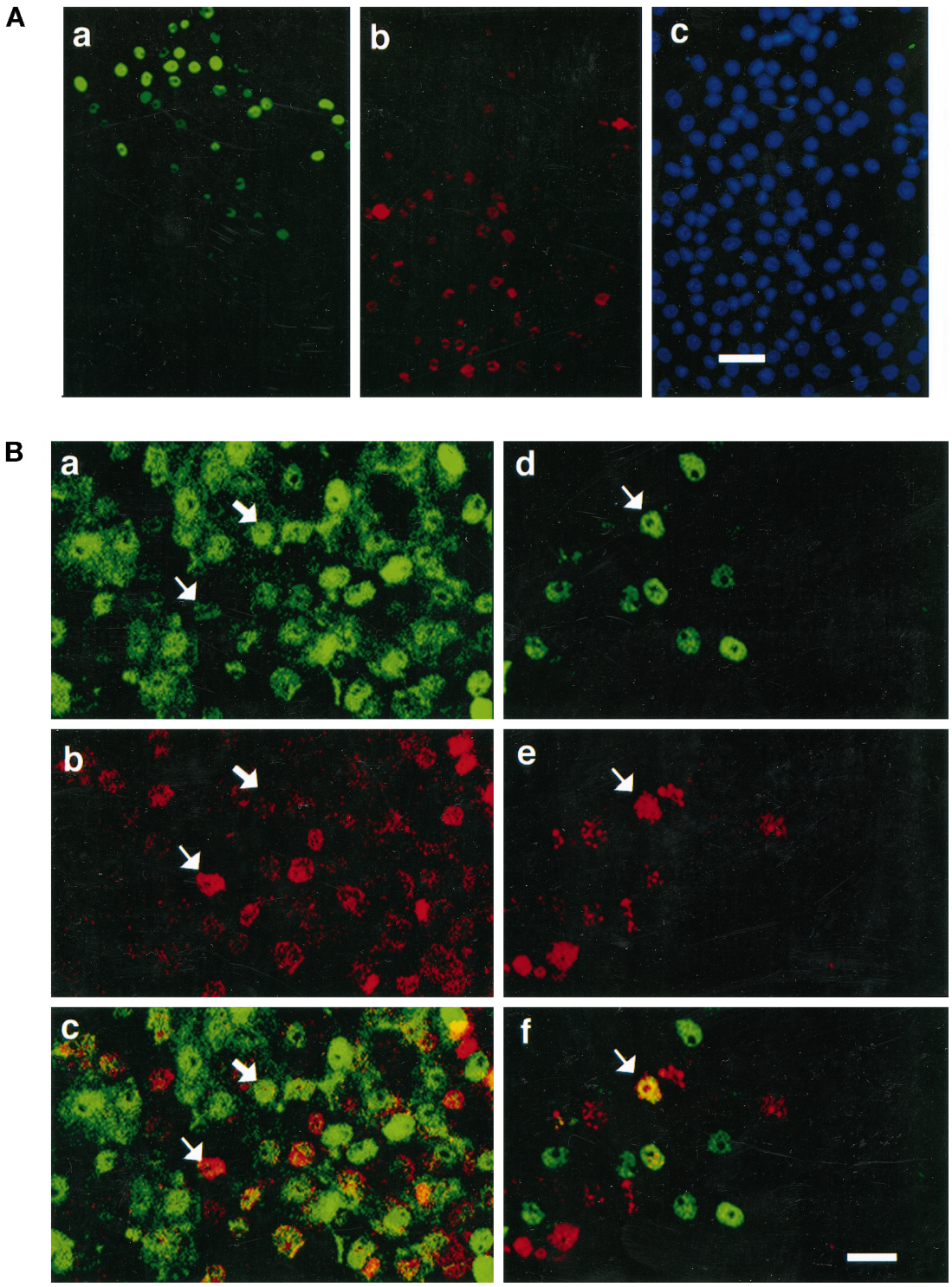


**Figure 8.** Fluorescence micrographs of deferoxamine-treated 8-d corneal epithelial cells, transferred to high-iron medium for 16 h, followed by 5 min of UV irradiation and, 4 h later, fixation. These cells were then triple labeled for nuclear ferritin by immunofluorescence (fluorescein), for DNA breaks by ISEL (rhodamine), and for cell nuclei with Hoechst dye (blue). The top three panels (Figure 8A, a–c) show each of these individual reactions in a region in which there is essentially a complete separation of the cells with nuclear ferritin and the cells with DNA breaks (Bar, 40 $\mu$m). The bottom (Figure 8B) shows two separate areas (panels a–c and d–f) selected for having some cells with both nuclear ferritin and nuclear breaks, seen most advantageously with the signals combined (panels c and f). As described in the text, the cells with weak signals for ferritin, in general, show strong signals for DNA breaks (a, b, and c, thin arrows) and vice versa (a, b, and c, thick arrows), with only an occasional cell showing appreciable signals for both (arrows in d, e, and f). Bar, 20 $\mu$m.

### *UV-induced DNA Strand Breaks*

Although the maximum damage to DNA occurs at 260 nm (within the UV-C spectrum), all wavelengths of UV light may induce the formation of thymine dimers and pyrimidine-pyrimidone (6–4) photoproducts (Matsunaga *et al.*, 1991). Pertinent to the current studies, all three wavelengths of UV light can induce the intracellular production of AOS (Yamanashi *et al.*, 1979; Black, 1987). UV-induced AOS damage to DNA includes base and deoxyribose damage, strand breaks, and DNA cross-linking (Halliwell and Aruoma, 1991; Janssen *et al.*, 1993). Such UV-induced DNA damage activates an excision-repair system in which the damaged bases are removed by endonuclease/exonuclease activity (Grossman *et al.*, 1988; Janssen *et al.*, 1993). This temporally leaves DNA breaks that can be detected by ISEL, the method chiefly employed in the current studies.

It is generally thought that only insignificant amounts of UV-C reach the earth's surface, due to filtration by the ozone layer. However, this may change due to fluorocarbon-induced ozone depletion. UV-B and UV-A do reach the earth's surface, and presently constitute a major environmental UV insult to the corneal epithelial cells (Pitts *et al.*, 1987; Bromidge *et al.*, 1995). In experimental situations, however, UV-C is at least one order of magnitude more efficient than UV-B at inducing DNA damage (Kodama *et al.*, 1984). Therefore, in the current studies, we employed UV-C irradiation (254 nm).

Consistent with other studies (Pitts *et al.*, 1987; Bromidge *et al.*, 1995), the UV-C irradiation induced dose-dependent DNA strand breaks in all cell types tested. However, the cell types showed different sensitivities to UV. Skin epithelial cells (keratinocytes) were the most sensitive; corneal and skin fibroblasts had intermediate sensitivities, and the corneal epithelial cells were the least sensitive. In addition, the appearance of DNA breaks in corneal epithelial cells had a considerable lag time, compared with the other cell types. These data are consistent with in vivo studies in which monkey eyes were exposed to UV-B (Pitts *et al.*, 1987). The damage to the cornea was dose-dependent, as determined by electron microscopy, and the corneal epithelial cells, but not the stromal fibroblasts, recovered completely.

The susceptibility of the skin epithelial cells to UV-induced DNA damage may provide a partial explanation for the high incidence of skin cancers. Conversely, cancers of the corneal epithelium are virtually nonexistent (Smolinand and Thoft, 1987).

### *Free Iron Exacerbates UV-induced DNA Damage*

The mechanism by which free iron generates AOS is by catalyzing the Fenton reaction via redox cycling within the cells (Stohs and Bagchi, 1995). Free iron as $Fe^{++}$ is the catalytically active form; $Fe^{+++}$ is largely inactive due to its low solubility at neutral pH. $Fe^{++}$ catalyzes the conversion of hydrogen peroxide ($H_2O_2$) and superoxide ($O_2^-$) to the hydroxyl radical (OH ·) which is the most reactive AOS (Janssen *et al.*, 1993). Therefore, to balance cellular needs with potential toxicity, iron must be finely controlled.

The Fenton reaction has been shown to increase hydrogen peroxide-produced DNA breaks in preparations of nuclei from human fibroblasts (Mello-Filho and Meneghini, 1984, 1991) and rat hepatocytes (Shires, 1982). Low-intensity UV-A-induced damage to DNA is strongly enhanced in the Fenton reaction system containing $Fe^{++}$ and $H_2O_2$ (Shih and Hu, 1996). Conversely, iron chelators protect DNA from hydrogen peroxide damage (Mello-Filho and Meneghini, 1984).

We observed that elevated iron dramatically increased UV-induced damage to DNA in corneal and skin fibroblasts (see also Audic and Giacomoni, 1993), but not in corneal epithelial cells. The enhancement of UV-induced DNA damage by iron could be direct, since iron–DNA complexes increase photon absorption (Audic and Giacomoni, 1993). However, it is more likely that this effect involves the iron-catalyzed oxidative damage to DNA, as suggested by others (Audic and Giacomoni, 1993; Shih and Hu, 1996).

### *Nuclear Ferritin and the Prevention of UV-induced DNA Damage*

Cells have evolved many protective mechanisms against oxidative damage (Audic and Giacomoni, 1993; Janssen *et al.*, 1993). A growing body of evidence suggests that the ferritin-mediated sequestration of iron is one of these (Balla *et al.*, 1992, 1993; Vile *et al.*, 1994) and that other iron-binding proteins, such as lactoferrin (Shimmura *et al.*, 1996), function similarly.

In the present studies, we observed that corneal epithelial cells in which the expression of nuclear ferritin was blocked showed a fivefold increase in DNA breaks when tested in an iron-containing environment. Several control experiments argue that this enhanced DNA damage did not result from any toxicity of deferoxamine, the iron chelator used to block the expression of nuclear ferritin. First, this inhibition of nuclear ferritin expression was reversed upon transferring the cells to iron-containing medium. Second, in deferoxamine-containing cultures, the de novo appearance of keratin 3 (K3), a differentiation marker for this cell type, was unaffected (Cai *et al.*, 1997). Most importantly, the difference in UV-induced DNA damage was not seen in cells UV-irradiated immediately or 2 h after deferoxamine or deferoxamine plus ferrous sulfate treatments. In both conditions free iron would have been sequestered—by chelation in the deferoxamine cultures and by ferritin sequestration in

the deferoxamine plus ferrous sulfate cultures (also described in RESULTS).

In our model of DNA protection, most likely it is the apoferritin or low-iron–containing forms of the nuclear molecule that would have the greatest effect. When corneal epithelial cells were cultured from an embryonic stage that already had nuclear ferritin (12–14 d), they showed no increase in UV-induced damage when tested in high-iron medium. When the cells were cultured from an embryo that had not yet initiated nuclear ferritin in vivo (7–8 d) but precociously expressed the molecule in vitro, an increase in DNA breaks was observed in high-iron medium, albeit slight. One possible explanation for this difference is that the nuclear ferritin synthesized in response to high iron may already be partially saturated with iron. Thus, while still protective, it is not as efficient as the molecule produced in vivo by the epithelial cells (see below).

When all of the experiments are considered, it seems that the protection afforded by the nuclear ferritin can be affected by two interrelated parameters. One is the total content of nuclear ferritin, and the other, as suggested above, is the degree of iron saturation. An effect of total ferritin concentration was seen in the experiment in which cells were examined by double-labeling for ferritin content and UV-induced nuclear damage. The results clearly showed a trend in which the cells that expressed the most nuclear ferritin showed the least damage to their DNA. That iron-saturated ferritin may have a diminished protective value, as discussed above, is consistent with recent studies on another iron-binding protein, lactoferrin. Lactoferrin is a component of tears, which, when saturated with iron, not only loses its protective effect against oxidative damage, but becomes toxic to cells (Shimmura *et al.*, 1996).

Consistent with this hypothesis, our preliminary evaluation of cellular iron by Prussian blue histochemistry produced no detectable signal in corneal epithelial cells, but did in liver and heart from the same aged embryos. Recent studies have demonstrated that thyroxine can up-regulate ferritin expression in rat hepatocytes (Leedman *et al.*, 1996). We also have obtained preliminary evidence that during development it is this hormone, rather than elevated iron, that is most likely to be responsible for the appearance of nuclear ferritin. These results are consistent with the nuclear ferritin in corneal epithelial cells being largely in the apoferritin form and thus capable of efficiently sequestering iron.

## ACKNOWLEDGEMENTS

We thank Drs. John Fitch and Marion Gordon for their helpful discussions and comments on the manuscript. We also thank Eileen Gibney and Emanuel Zycband for their technical assistance. This work was supported by NIH grants EY05191 (to T.F.L.) and EY05129 (to D.E.B.).

## REFERENCES

Audic, A., and Giacomoni, P.U. (1993). DNA nicking by ultraviolet radiation is enhanced in the presence of iron and of oxygen. Photochem. Photobiol. *57*, 508–512.

Balla, J., Jacob, H.S., Balla, G., Nath, K., Eaton, J.W., and Vercellotti, G.M. (1993). Endothelial-cell heme uptake from heme proteins: induction of sensitization and desensitization to oxidant damage. Proc. Natl. Acad. Sci. USA *90*, 9285–9289.

Balla, G., Jacob, H.S., Balla, J., Rosenberg, M., Nath, K., Apple, F., Eaton, J.W., and Vercellotti, G.M. (1992). Ferritin: a cytoprotective antioxidant strategem of endothelium. J. Biol. Chem. *267*, 18148–18153.

Black, H.S. (1987). Potential involvement of free radical reactions in ultraviolet light-mediated cutaneous damage. Photochem. Photobiol. *46*, 213–221.

Bromidge, T.J., Howe, D.J., Johnson, S.A., and Phillips, M.J. (1995). Adaptation of the TdT assay for semi-quantitative flow cytometric detection of DNA strand breaks. Cytometry *20*, 257–260.

Cai, C.X., Birk, D.E., and Linsenmayer, T.F. (1997). Ferritin is a developmentally-regulated nuclear protein of avian corneal epithelial cells. J. Biol. Chem. *272*, 12831–12839.

Cerutti, P.A. (1985). Prooxidant states and tumor promotion. Science *227*, 375–381.

Coates, P.J., Save, V., Ansari, B., and Hall, P.A. (1995). Demonstration of DNA damage/repair in individual cells using in situ end labelling: association of p53 with sites of DNA damage. J. Pathol. *176*, 19–26.

Gedik, C.M., Ewen, S.W., and Collins, A.R. (1992). Single-cell gel electrophoresis applied to the analysis of UV-C damage and its repair in human cells. Int. J. Radiat. Biol. *62*, 313–320.

Grossman, L., Caron, P.R., Mazur, S.J., and Oh, E.Y. (1988). Repair of DNA-containing pyrimidine dimers. FASEB J. *2*, 2696–2701.

Halliwell, B., and Aruoma, O.I. (1991). DNA damage by oxygen-derived species. Its mechanism and measurement in mammalian systems. FEBS Lett. *281*, 9–19.

Hart, R.W., Setlow, R.B., and Woodhead, A.D. (1977). Evidence that pyrimidine dimers in DNA can give rise to tumors. Proc. Natl. Acad. Sci. USA *74*, 5574–5578.

Janssen, Y.M., Van Houten, B., Borm, P.J., and Mossman, B.T. (1993). Cell and tissue responses to oxidative damage. Lab. Invest. *69*, 261–274.

Kodama, K., Ishikawa, T., and Takayama, S. (1984). Dose response, wavelength dependence, and time course of ultraviolet radiation-induced unscheduled DNA synthesis in mouse skin in vivo. Cancer Res. *44*, 2150–2154.

Leedman, P.J., Stein, A.R., Chin, W.W., and Rogers, J.T. (1996). Thyroid hormone modulates the interaction between iron regulatory proteins and the ferritin mRNA iron-responsive element. J. Biol. Chem. *271*, 12017–12023.

Liu, Z.G., Baskaran, R., Lea-Chou, E.T., Wood, L.D., Chen, Y., Karin, M., and Wang, J.Y. (1996). Three distinct signalling responses by murine fibroblasts to genotoxic stress. Nature *384*, 273–276.

Lu, X., and Lane, D.P. (1993). Differential induction of transcriptionally active p53 following UV or ionizing radiation: defects in chromosome instability syndromes? Cell *75*, 765–778.

Matsunaga, T., Hieda, K., and Nikaido, O. (1991). Wavelength dependent formation of thymine dimers and (6–4) photoproducts in

DNA by monochromatic ultraviolet light ranging from 150 to 365 nm. Photochem. Photobiol. *54*, 403–410.

Mello-Filho, A.C., and Meneghini, R. (1984). In vivo formation of single-strand breaks in DNA by hydrogen peroxide is mediated by the Haber-Weiss reaction. Biochim. Biophys. Acta *781*, 56–63.

Mello-Filho, A.C., and Meneghini, R. (1991). Iron is the intracellular metal involved in the production of DNA damage by oxygen radicals. Mutat. Res. *251*, 109–113.

Pendrys, J.P. (1983). A model of the kinetics of photorepair in chick embryo fibroblasts. Mutat. Res. *122*, 129–133.

Pitts, D.G., Bergmanson, J.P., and Chu, L.W. (1987). Ultrastructural analysis of corneal exposure to UV radiation. Acta Ophthalmol. *65*, 263–273.

Schmid, T.M., and Linsenmayer, T.F. (1985). Immunohistochemical localization of short chain cartilage collagen (type X) in avian tissues. J. Cell Biol. *100*, 598–605.

Shih, M.K., and Hu, M.L. (1996). UVA-potentiated damage to calf thymus DNA by Fenton reaction system and protection by para-aminobenzoic acid. Photochem. Photobiol. *63*, 286–291.

Shimmura, S., Suematsu, M., Shimoyama, M., Tsubota, K., Oguchi, Y., and Ishimura, Y. (1996). Subthreshold UV radiation-induced peroxide formation in cultured corneal epithelial cells: the protective effects of lactoferrin. Exp. Eye Res. *63*, 519–526.

Shires, T.K. (1982). Iron-induced DNA damage and synthesis in isolated rat liver nuclei. Biochem. J. *205*, 321–329.

Smolinand, G., and Thoft, R.A. (1987). The Cornea: Scientific Foundations and Clinical Practice, Boston/Toronto: Little, Brown and Company.

Spurr, S.J., and Gipson, I.K. (1985). Isolation of corneal epithelium with dispase II or EDTA: effects on the basement membrane zone. Invest. Ophthalmol. & Visual Sci. *26*, 818–827.

Stohs, S.J., and Bagchi, D. (1995). Oxidative mechanisms in the toxicity of metal ions. Free Radical Biol. & Med. *18*, 321–336.

Vile, G.F., Basu-Modak, S., Waltner, C., and Tyrrell, R.M. (1994). Heme oxygenase 1 mediates an adaptive response to oxidative stress in human skin fibroblasts. Proc. Natl. Acad. Sci. USA *91*, 2607–2610.

Yamanashi, B.S., Hacker, H., and Klintworth, G.K. (1979). Wavelength dependence and kinetics of UV-induced free radical formation in the human cornea and lens. Photochem. Photobiol. *30*, 391–395.

Zak, N.B., and Linsenmayer, T.F. (1983). Monoclonal antibodies against developmentally regulated corneal antigens. Dev. Biol. *99*, 373–381.